

The Amidohydrolases IAR3 and ILL6 Contribute to Jasmonoyl-Isoleucine Hormone Turnover and Generate 12-Hydroxyjasmonic Acid Upon Wounding in *Arabidopsis* Leaves^{*S}

Received for publication, July 5, 2013, and in revised form, September 9, 2013. Published, JBC Papers in Press, September 19, 2013, DOI 10.1074/jbc.M113.499228

Emilie Widemann^{‡S1}, Laurence Miesch[¶], Raphaël Luga[§], Emilie Holder[¶], Clément Heinrich[¶], Yann Aubert[‡], Michel Miesch[¶], Franck Pinot[§], and Thierry Heitz^{‡2}

From the [‡]Institut de Biologie Moléculaire des Plantes, Unité Propre de Recherche 2357 du Centre National de la Recherche Scientifique, Université de Strasbourg, 12 rue du Général Zimmer, 67084 Strasbourg Cedex, France, the [§]Institut de Biologie Moléculaire des Plantes, Unité Propre de Recherche 2357 du Centre National de la Recherche Scientifique, Université de Strasbourg, 28 rue Goethe, 67083 Strasbourg Cedex, France, and the [¶]Laboratoire de Chimie Organique Synthétique, Institut de Chimie, Unité Mixte de Recherche 7177, Université de Strasbourg, Centre National de la Recherche Scientifique, 1 rue Blaise Pascal, 67008 Strasbourg Cedex, France

Background: The plant hormone jasmonoyl-isoleucine (JA-Ile) undergoes oxidative catabolism mediated by cytochrome P450 enzymes.

Results: Two amidohydrolases catalyze the cleavage of JA-Ile conjugates and generate 12OH-JA during *Arabidopsis* wound response.

Conclusion: IAR3 and ILL6 define an additional pathway for JA-Ile turnover and establish a biosynthetic route for 12OH-JA.

Significance: New enzymatic steps unravel the complexity in jasmonate metabolism.

Jasmonates (JAs) are a class of signaling compounds that mediate complex developmental and adaptive responses in plants. JAs derive from jasmonic acid (JA) through various enzymatic modifications, including conjugation to amino acids or oxidation, yielding an array of derivatives. The main hormonal signal, jasmonoyl-L-isoleucine (JA-Ile), has been found recently to undergo catabolic inactivation by cytochrome P450-mediated oxidation. We characterize here two amidohydrolases, IAR3 and ILL6, that define a second pathway for JA-Ile turnover during the wound response in *Arabidopsis* leaves. Biochemical and genetic evidence indicates that these two enzymes cleave the JA-Ile signal, but act also on the 12OH-JA-Ile conjugate. We also show that unexpectedly, the abundant accumulation of tuberonic acid (12OH-JA) after wounding originates partly through a sequential pathway involving (i) conjugation of JA to Ile, (ii) oxidation of the JA-Ile conjugate, and (iii) cleavage under the action of the amidohydrolases. The coordinated actions of oxidative and hydrolytic branches in the jasmonate pathway highlight novel mechanisms of JA-Ile hormone turnover and redefine the dynamic metabolic grid of jasmonate conversion in the wound response.

Recent years have seen significant progress in our understanding of how hormonal pathways orchestrate plant development and their adaptation to environmental cues. This is particularly the case for jasmonates (JAs),³ a term that refers to jasmonic acid (JA) and its derivatives, for which mechanistic insights into the biosynthesis, perception/action, and modification have been reported (1, 2).

JAs regulate important steps in plant development, but their roles are best documented as mediators of inducible responses to herbivorous insects and necrotrophic pathogens (3–5). These aggressors trigger the JA pathway, which in turn up-regulates overlapping yet distinct sets of genes that lead to the accumulation of a specific arsenal of chemical defenses and proteins (6, 7). Jasmonate metabolism is strongly stimulated by mechanical leaf wounding in *Arabidopsis* (8, 9) and in other plant species, and triggers many responses induced by leaf-eating insects (10).

The processes and enzymes leading to jasmonic acid (JA) biosynthesis are relatively well described (2), but the nature of the initial molecular event triggering the pathway is still elusive. In *Arabidopsis*, partially redundant lipases release the precursor fatty acid α -linolenic acid from plastidial membranes where it is converted to 12-oxo-phytodienoic acid through the sequential action of 13-lipoxygenases, the cytochrome P450 allene oxide synthase, and allene oxide cyclase. 12-Oxo-phytodienoic acid is then translocated to peroxisomes where it is reduced by 12-oxo-phytodienoic acid reductase 3 before three

* This work was supported in part by Agence Nationale de la Recherche Contract ANR-12-BSV8-005 (to Y. A.).

^S This article contains supplemental Methods S1.

¹ Supported by a doctoral fellowship from the Ministère de l'Enseignement Supérieur et de la Recherche.

² To whom correspondence should be addressed: Institut de Biologie Moléculaire des Plantes, Centre National de la Recherche Scientifique, 12 rue du Général Zimmer 67084 Strasbourg Cedex, France. Fax: 33-388614442; E-mail: thierry.heitz@ibmp-cnrs.unistra.fr.

³ The abbreviations used are: JA, jasmonates or jasmonic acid; TA, tuberonic acid; JA-Ile, (+)-7-iso-jasmonoyl-L-isoleucine; JAR1, JASMONATE RESISTANT 1; COI1, CORONATINE INSENSITIVE 1; JAZ, Jasmonate ZIM domain; IAA-Ala, indole acetic acid-alanine; UPLC, ultra performance liquid chromatography; ANOVA, analysis of variance; qPCR, quantitative PCR.

Jasmonate Conjugate Cleavage and Tuberonic Acid Formation

rounds of β -oxidation of the side chain. JA has been viewed initially as the active jasmonate in plants, due to its abundance and relative stability, and also because JA treatment recapitulates most known jasmonate responses.

JA is subjected to many enzymatic modifications that generate an array of derivatives, including oxidized and/or sulfonated forms or amino acid or sugar conjugates (2, 11). These individual jasmonates vary in abundance, biological activity, and distribution under various stimuli and in different tissues. For example, the JA metabolite 12OH-JA was first described in potato and *Solanaceous* species for its tuber-inducing activity, hence its trivial name tuberonic acid (TA) (12). More recently, TA and its sulfonated or glucosylated derivatives were found as commonly occurring metabolites of JA, particularly in the wound response (13, 14), but the mode of formation of TA and biological activity of its derivatives are still largely unknown. TA formation has, however, been proposed as a partial switch-off in JA signaling (14). However, TA could also be a metabolic intermediate, for example, TA-glucoside was described as a specific signal triggering leaf closing in the rain tree *Samanea saman* (15).

Among many existing JA modification routes, the JASMONATE RESISTANT 1 (JAR1)-catalyzed formation of (+)-7-*iso*-jasmonoyl-L-isoleucine (JA-Ile) is the critical signal activation step (16). JAR1 is a member of the GH3 family of acyl amidosynthases, whose other described members conjugate auxin to amino acids (17), indicating possible metabolic cross-talk between auxin and JA pathways. JA-Ile specifically promotes assembly of a co-receptor composed of the F-box protein CORONATINE INSENSITIVE 1 (COI1) and Jasmonate ZIM domain (JAZ) proteins. JAZ proteins constitute a family of transcriptional repressors that under low JA-Ile content prevent the transcription of target genes. JA-Ile-triggered co-receptor assembly results in JAZ ubiquitination by the SCF^{COI1} E3 ligase and their subsequent proteolytic removal by the 26S proteasome, leading to the derepression of target genes, and the deployment of the JA response (18, 19).

Plants have also evolved mechanisms to reset JA signaling to pre-stimulation conditions. For example, the strong JAZ repressor gene co-induction with the JA metabolic pathway is believed to rapidly restore a repressed state on JA-responsive promoters (10). Another means to terminate signaling is to modify or eliminate the hormonal signal. We and others have recently described a cytochrome P450 (CYP)-based catabolic pathway that contributes to the turnover of JA-Ile. CYP94B3 and CYP94C1 oxidize JA-Ile at the C12 position, leading to sequential accumulation of the oxidized derivatives 12OH-JA-Ile and 12COOH-JA-Ile (20–22). This oxidative metabolism accounts largely for the transient nature of JA-Ile accumulation after wounding and, similarly to other plant hormones (23), corresponds to the attenuation of the hormonal signal, as plants with perturbed JA-Ile oxidizing activity have an altered JA response (20, 22).

Phytohormone conjugation to amino acids is generally associated with storage or inactivation purposes (24) like in the case of auxin, but the fascinating counter example of JA-Ile activity suggests that de-conjugation could be used to readily inactivate

this hormone. Gene families encoding auxin amidohydrolases and their regulation by interacting microorganisms have been described in *Brassica rapa* (25) and *Medicago truncatula* (26). In *Arabidopsis*, they form a 7-gene family (*IAR3*, *ILL1*, *ILL2*, *ILL3*, *ILL5*, *ILL6*, and *ILR1*) with several members known to cleave auxin-amino acid conjugates (27). *IAR3*, encoding an indole acetic acid-alanine (IAA-Ala) hydrolase (28), was initially described as a wound- and jasmonate-induced gene named Jasmonate Responsive 3 (*JR3*) and used as a robust JA pathway marker (29). Recently, Woldemariam *et al.* (40) reported the characterization of the *IAR3*-related jasmonoyl-isoleucine hydrolase 1 (*JIH1*), an herbivore-induced amidohydrolase from the wild species *Nicotiana attenuata*, which contributes to JA-Ile signal attenuation by cleaving the hormone into JA and Ile. We describe here the characterization of *IAR3* and *ILL6*, two of three amidohydrolase genes that are co-regulated with the JA pathway in *Arabidopsis*. *IAR3* was previously characterized in the context of auxin conjugate hydrolysis (28), but no data were available for *ILL6*. Starting from a metabolic analysis of several JA pathway mutants, we hypothesized the action of amidohydrolases to explain the particular jasmonate profiles in these lines. Indeed, recombinant *IAR3* and *ILL6* were found to cleave JA-Ile *in vitro*, consistent with a role in hormonal turnover upon wounding. Interestingly, the enzymes also seem to act on the hydroxylated JA-Ile conjugate, with important consequences on the homeostasis of oxidized jasmonates. Particularly, we elucidate an unexpected mode of TA formation that, instead of direct hydroxylation of JA, proceeds through the cleavage of JAR1- and CYP94-generated 12OH-JA-Ile.

EXPERIMENTAL PROCEDURES

Plant Growth and Treatment—*Arabidopsis thaliana* genotypes used were all in the Col0 ecotype and grown under a 12/12-h photoperiod in a growth chamber. T-DNA insertion lines used were: *coi1-1*, *jar1-1*, the double mutant between *cyp94c1-1* (SALK_55455) and *cyp94b3-1* (CS302217) described in Ref. 20, *iar3-5* (SALK_069047), *iar3-6* (SALK_042101), *ill6-1* (GK412E11), and *ill6-2* (SALK_024894), all obtained from the Nottingham Arabidopsis Stock Center (NASC). For wounding experiments, between 4 and 6 fully expanded leaves of 6–7-week-old plants were wounded three times across the midvein with a hemostat. At increasing time points following mechanical damage, leaf samples were quickly harvested and flash-frozen in liquid nitrogen before storing at -80°C until use.

RT-Quantitative PCR (qPCR) Gene Expression Assays—Total RNA was extracted from plant leaves with TRIzol reagent (Molecular Research Center). One μg of RNA was reverse transcribed using the ImProm-II reverse transcription system (Promega, Madison, WI). Real-time PCR was performed on 10 ng of cDNA as described in Ref. 30 using a LightCycler 480 II instrument (Roche). The housekeeping genes *EXP* (At4g26410) and *GAPDH* (At1g13440) were used as internal references. *GAPDH* was replaced by *At4g26410* encoding an unknown protein (31) in the experiments with *coi1* plants. Gene-specific primer sequences used for qPCR are listed in Table 1.

Chemical Synthesis of Oxidized Jasmonates—JA-Ile was obtained according to the reported method (32). 12-OH-JA-Me-Ile was obtained as described in Refs. 21 and 33. The

TABLE 1
Primers used in this study

Use	Gene/allele (locus)	Primer name	Sequence (5' → 3')
qPCR	<i>CYP94B1</i> (At5g63450)	CYP94B1 qPCR F62	caatgaggctttaccaccag
		CYP94B1 qPCR R62	aaatgtcgtctgtttgtcat
	<i>CYP94B3</i> (At3g48520)	CYP94B3 qPCR F62	tggttacacgaaggctgtc
		CYP94B3 qPCR R62	agtcccacgaataggagat
	<i>CYP94C1</i> (At2g27690)	CYP94C1 qPCR F63	ggccggattacgaagattt
		CYP94C1 qPCR R63	ggccggaacttacctcgtt
	<i>IAR3</i> (At1g51760)	IAR3 qPCR-F	gggtgatgatgatgacattg
		IAR3 qPCR-R	tgcatcttccctggaacctt
		IAR3-69047-qF ^a	ttgcttctgtaccctgct
		IAR3-69047-qR ^a	tcgataagcaagtgaaagga
	<i>ILL1</i> (At5g56650)	ILL1 qPCR-F	tcaacaacatcgccaacatt
		ILL1 qPCR-R	caacgttctcaacgtcct
	<i>ILL2</i> (At5g56660)	ILL2 qPCR-F	atgaacatcgccaccattg
		ILL2 qPCR-R	ctcatcttctgtccactcaa
	<i>ILL3</i> (At5g54140)	ILL3 qPCR-F	tggtgctcccgctgctgata
		ILL3 qPCR-R	ttgtcttatgatccactcaa
	<i>ILL5</i> (At1g51780)	ILL5 qPCR-F	gtttcacgagaggcagatcct
		ILL5 qPCR-R	tcgggaatgacattaaagca
	<i>ILL6</i> (At1g44350)	ILL6 qPCR-F	ggctgataggacgactacc
		ILL6 qPCR-R	tgcatcttgcctgcaacttt
	ILL6-GK412-F ^a	gtgtccatcatccaacggt	
	ILL6-GK412-R ^a	ggtccgacataccatgatcc	
	ILL6-024894-F ^a	cttggtgctgccatattct	
	ILL6-024894-R ^a	Tcatcaaaagctcctgcttc	
	<i>ILR1</i> (At3g02875)	ILR1 qPCR-F	Actggatccactcgaagctg
	ILR1 qPCR-R	Tgcggtattacgttttgagca	
<i>ST2a</i> (At5g07010)	ST2a qPCR-F	Ggcttgcaacttcttagagctt	
	ST2a qPCR-R	Cggcgatagccttcacaac	
<i>EXP</i> (At4g26410)	EXP-qPCR-F	Gagctgaagtggcttcaatgac	
	EXP-qPCR-R	Ggtccgacataccatgatcc	
	<i>GAPDH</i> (At1g13440)	GAPDH-qPCR-F	Tgggtgacaacaggtcaagca
	GAPDH-qPCR-R	Aaactgtgctcaatgcaatc	
	<i>At4g26410</i>	At4g26410-qPCR-F	Gagctgaagtggcttccatgac
		At4g26410-qPCR-R	Ggtccgacataccatgatcc
<i>IAR3</i> and <i>ILL6</i> cloning in pENTR1a for recombinant protein expression	<i>IAR3</i>	Sall-IAR3ΔN-F EcoRI-IAR3ΔN-R	Ctggctgactcctctaagggttatctcaaatc Tgtgaattcaaagttcatctttttgtactct
	<i>ILL6</i>	Sall-ILL6ΔN-F EcoRI-ILL6ΔN-R	Gtggctgcacccaacttaccttcttgaagtg Caagaattcttgaatgtttatcatttaagtatctc
T-DNA genotyping	T-DNA	LbB1.3 (SALK)	Attttgcggatttcgaac
	<i>iar3-5</i>	o8409 (GABI-Kat)	Atattgaccatcactactcattgc
		SALK_069047-LP	Gttctccacgtgcgttatagc
		SALK_069047-RP	Aaaaagccacactgttccatg
	<i>iar3-6</i>	SALK_042101-LP	Gttctccacgtgcgttatagc
		SALK_042101-RP	Acaccagtaacagcaactggg
	<i>ill6-1</i>	GK412E11-LP	Gactatgcttcttggtgctgc
	GK412E11-RP	Cgcaccttgaatcgtttc	
<i>ill6-2</i>	SALK_024894-LP	Gactatgcttcttggtgctgc	
	SALK_024894-RP	Cgcaccttgaatcgtttc	

^a Primers used for *iar3* and *ill6* T-DNA lines.

hydroxyl group and carboxyl function of 12OH-JA-Me-Ile were successively protected to provide 12-OAc-dioxaspiro-JA-Me-Ile. After saponification of the latter, the primary alcohol was oxidized using tetrapropylammonium perruthenate-*N*-methylmorpholine-*N*-oxide (34). Deprotection of the dioxolane function afforded 12COOH-JA-Me-Ile. Saponification of the carbomethoxy group was achieved using Me₃SnOH (35) to yield the desired 12-COOH-JA-Ile. The complete procedures, the characterization of intermediates, and final product are given in supplemental Methods S1.

Recombinant IAR3 and ILL6 Production and Enzymatic Hydrolase Assay—For heterologous expression of IAR3 and ILL6, open reading frame sequences deleted of the 25 N-terminal signal peptide-encoding codons were amplified using Phusion *Taq* Polymerase (Thermo Scientific) prior to cloning in the pENTR1a (Invitrogen) plasmid in the DH5α *Escherichia coli* strain. Inserts with error-free sequences were recombined into

the expression vector pHMWGA using GatewayTM technology (Invitrogen). Plasmids were further transformed into *E. coli* SoluBL21 strain (AMS Biotechnology, Abingdon, UK). Ice-cold bacterial pellets from isopropyl 1-thio-β-D-galactopyranoside-induced cultures were collected and resuspended in lysis buffer (50 mM Tris-HCl, pH 8, 300 mM NaCl, 5% glycerol, 1 mg/ml of lysozyme, 1 mM PMSF, 1 mM EDTA, 0.1% Tween 20) at an A₆₀₀ of 20. Bacteria were lysed by sonication on ice for 2 min. Clarified protein lysates were filtered and loaded on a 1-ml HisTrap HP column (GE Healthcare Bio-Sciences) equilibrated in 50 mM Tris-HCl, pH 8, 300 mM NaCl, 5% glycerol installed on an Äkta Purifier10 Liquid chromatography system. The column was washed with equilibration buffer and bound protein was eluted with equilibration buffer complemented with 500 mM imidazole. Eluate was desalted on PD10 columns and the protein concentration was determined by polyacrylamide gel electrophoresis using a bovine serum albumin standard series.

Jasmonate Conjugate Cleavage and Tuberonic Acid Formation

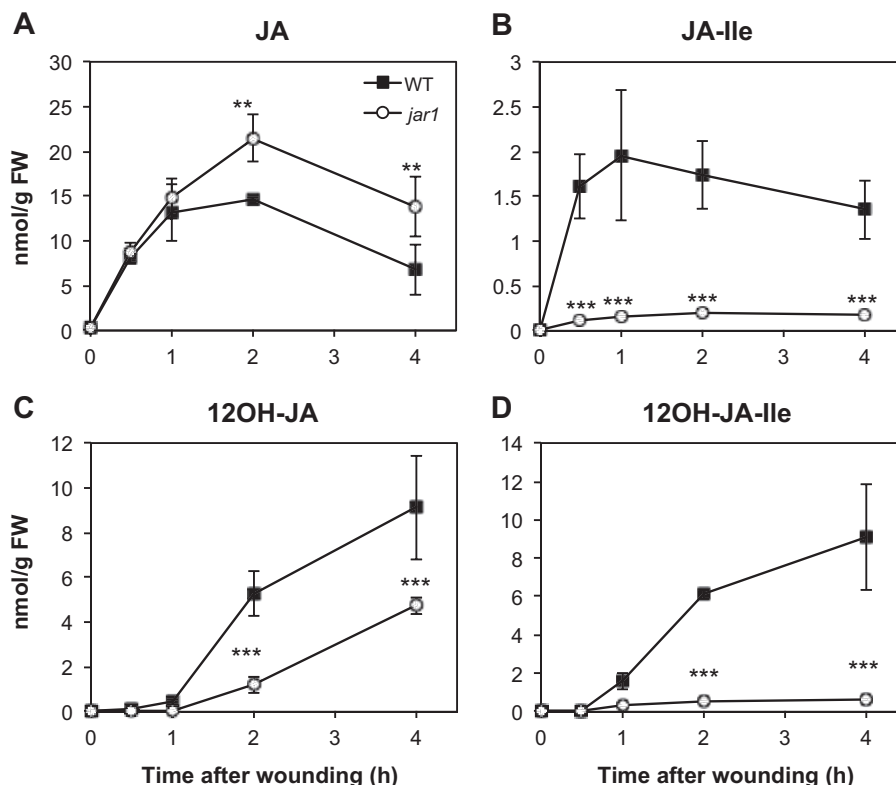


FIGURE 1. Kinetic analysis of jasmonate accumulation in wild-type (WT) and in *jar1* mutant plants upon leaf wounding. Leaves were harvested at increasing times after wounding and extracted for jasmonate determination by UPLC-MS/MS. A, JA; B, JA-Ile; C, 12OH-JA; D, 12OH-JA-Ile. Data are mean \pm S.E. from three biological samples. Asterisks indicate significant differences between mutant and WT at $p < 0.01$ (**) or $p < 0.001$ (***) (two-way ANOVA). Similar results were obtained in two independent experiments.

Incubation conditions were based on those described for IAR3 activity with IAA-Ala (Sigma) (36). Incubations were performed in 200 μ l containing 50 mM Tris-HCl, pH 8, 1 mM MnCl₂, 1 mM dithiothreitol, and 50 μ M JA-Ile or 12OH-JA-Ile or 12COOH-JA-Ile synthesized as described in the previous section as substrate. Control reactions were run with a similar amount of purified maltose-binding protein. Reactions were incubated at 30 °C and stopped by addition of 40 μ l of 1 M HCl before extraction with 240 μ l of ethyl acetate. After brief vortexing and centrifugation, the upper organic phase was dried under N₂ flow, and reconstituted with 150 μ l of MeOH before UPLC-MS analysis as described below.

Jasmonate Profiling—Jasmonates were identified and quantified in plant extracts and enzymatic incubations by ultra performance liquid chromatography coupled to tandem mass spectrometry (UPLC-MS/MS), using MS transitions determined from pure standards (JA, 12OH-JA, JA-Ile, 12OH-JA-Ile, or 12COOH-JA-Ile). The relative quantification in samples was achieved by reporting MS peak areas relative to internal standard peak area and mass of biological material. Absolute quantifications of JA, 12OH-JA, JA-Ile, 12OH-JA-Ile, or 12COOH-JA-Ile were determined by comparison of a sample signal with dose-response curves established for each pure compound. For plant extraction, 5 volumes of ice-cold 90% methanol containing 9,10-dihydro-JA and 9,10-dihydro-JA-Ile as internal standards were added to one fresh weight (100–150 mg pre-weighed) of frozen leaf powder in a screw-capped tube containing glass beads. Material was ground twice for 30 s with a

Precellys 24 tissue homogenizer (Bertin Technologies, Montigny-Le-Bretonneux, France). Homogenates were cleared by two successive centrifugations at 20,000 \times g and supernatants were saved for UPLC-MS analysis. The conditions for analyzing jasmonates in enzymatic incubations or in plant extracts were described in Ref. 20. The multiple reaction monitoring transitions used for detection were (in negative mode): JA 209 > 59; 12OH-JA 225 > 59; 12OH-JA-Glc 387 > 89; 12-HSO₄-JA 305 > 97; 12OH-JA-Ile 338 > 130; 12COOH-JA-Ile 352 > 130; IAA-Ala 247 > 130 and in positive mode: JA-Ile 324 > 151, IAA 176 > 130.

Statistical Analysis—All statistical analysis were established by two-way ANOVA with Bonferroni post test using GraphPad Prism version 5.01.

RESULTS

Tuberonic Acid Abundance Is Not Correlated with JA Levels but with 12OH-JA-Ile Levels in JAR1- or CYP94B3/C1-deficient Plants Upon Wounding—12OH-JA (tuberonic acid, TA) as well as its glucoside (12-O-Glc-JA, TA-Glc) and its sulfated derivative 12-HSO₄-JA have been identified as common JA metabolites in several plant species (14). TA was further shown to accumulate in *N. attenuata* (37), tomato (14), and *Arabidopsis* (8) after leaf wounding. A kinetic analysis shows that TA is nearly undetectable in unstressed leaves and maximal levels are reached by 4 h after injury (Fig. 1C) in wild-type (WT) plants, which is later than those of JA that peak generally between 1 and 2 h (Fig. 1A). Despite the lack of data about TA biosynthesis, it

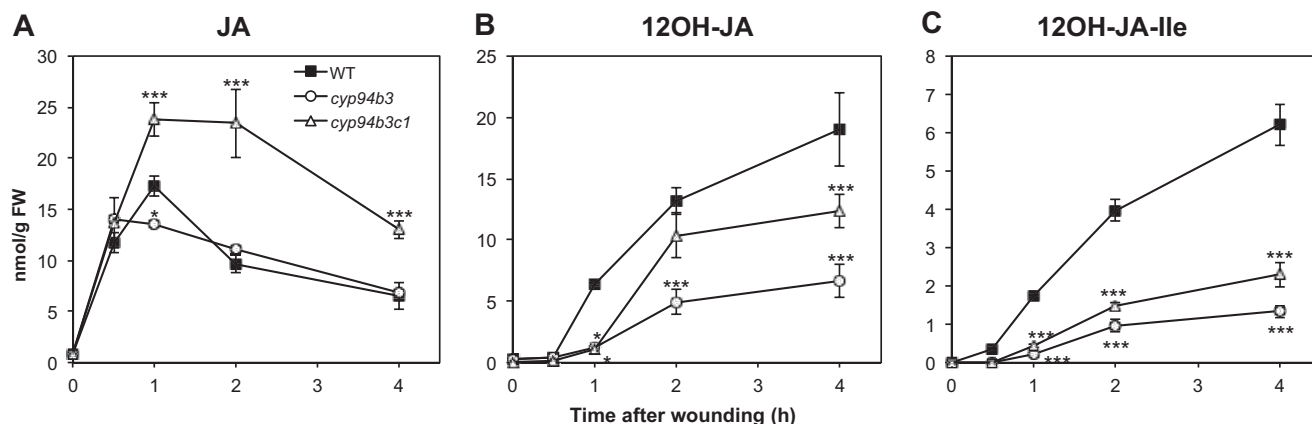


FIGURE 2. Kinetic analysis of hydroxylated jasmonate accumulation in wild-type (WT), *cyp94b3*, and *cyp94b3c1* mutant plants upon leaf wounding. Leaves were harvested at increasing times after wounding and extracted for jasmonate determination by UPLC-MS/MS. A, JA; B, 12OH-JA; C, 12OH-JA-Ile. Data are mean \pm S.E. from three biological samples. Asterisks indicate significant differences between mutant and WT at $p < 0.05$ (*) or $p < 0.001$ (***) (two-way ANOVA).

is commonly thought that TA formation occurs through JA hydroxylation. In the course of the characterization of the impact of JA conjugation on the accumulation of oxidized JA-Ile derivatives (20), we analyzed the jasmonate profiles in *jar1*, a mutant impaired in JA-Ile formation. Levels of JA were increased (Fig. 1A) and those of JA-Ile depressed (Fig. 1B) in wounded *jar1* compared with WT leaves, as expected for a block in JA-conjugating activity. Unexpectedly, despite JA overaccumulation, TA levels were reduced compared with WT (Fig. 1C). TA levels were severely reduced in *jar1* at 2 h post-wounding and did not exceed 50% WT levels at 4 h, suggesting that excess JA in *jar1* does not seem to function as a substrate for direct hydroxylation to form TA. Reduced TA levels were correlated with the strongly impaired accumulation of JA-Ile (Fig. 1B) and 12OH-JA-Ile (Fig. 1D). These observations suggest that the active hormone JA-Ile and/or the hydroxylated compound 12OH-JA-Ile are necessary for TA formation.

To determine which of these compounds is required for full TA accumulation, we examined the levels of TA in the *cyp94b3* and *cyp94b3c1* oxidation mutants in which JA-Ile is durably overaccumulated (20) and 12OH-JA-Ile is strongly reduced compared with WT (Fig. 2C). We observed in both mutants a significantly reduced build-up of TA (Fig. 2B), demonstrating that prolonged JA-Ile accumulation is not sufficient to achieve high TA levels when 12OH-JA-Ile levels are decreased, and arguing that 12OH-JA-Ile is a precursor for TA formation. This latter hypothesis is also supported by 12OH-JA-Ile levels in *cyp94b3c1*, exceeding levels in *cyp94b3* because of the impaired conversion to 12COOH-JA-Ile in the double mutant, which are correlated with commensurate effects on TA levels. Our previous *in vitro* data indicated that neither CYP94B3 nor CYP94C1 exhibited detectable JA-hydroxylase activity (20), therefore the reduced accumulation of TA in *cyp94b3* and *cyp94b3c1* mutants is unlikely due to a lack of CYP94-mediated JA hydroxylase activity. Similarly to *jar1*, JA is overaccumulated in *cyp94b3c1* (Fig. 2A), yet TA levels are lower than in WT (Fig. 2B).

Together, these metabolic studies in different genetic backgrounds indicate that a large part of TA accumulation is dependent on JAR1 conjugation and on CYP94 conjugate oxi-

dation activities, pointing to the hypothesis that 12OH-JA-Ile may be an important precursor for TA formation. This indirect evidence prompted us to investigate the missing step leading to the formation of TA, and namely to explore the possibility that it may proceed through cleavage of the 12OH-JA-Ile conjugate.

Several Amidohydrolase Genes Are Wound and COI1 Regulated in Arabidopsis—Woldemariam *et al.* (40) have recently described the herbivory-induced JIH amidohydrolase that cleaves JA-Ile to JA in *N. attenuata*. JIH defines an alternative JA-Ile hormone inactivation pathway that contributes to the attenuation of the JA-Ile burst. *Arabidopsis* possesses a family of 7 related amidohydrolases (36), with several members described as cleaving auxin conjugates (27, 28, 38). Recent large scale transcriptional analysis of public microarray data using co-regulation tools (39) revealed a strong coregulation of *IAR3*, *ILL5*, and *ILL6* with the jasmonate metabolic and signaling pathways (data not shown), which includes the two *CYP94* genes acting in JA-Ile catabolism (20–22). Experimental examination of the 7 gene expression profiles confirmed a rapid and transient wound induction of *IAR3*, *ILL5*, and *ILL6* transcripts (Fig. 3, A–C). Kinetics were typical of early responsive genes, peaking by 1–2 h, and largely paralleled those of *CYP94B1*, *CYP94B3*, and *CYP94C1* (20). The analysis also revealed the wound-responsive expression of *ILL1*, with a slight delay (Fig. 3D). Up-regulation of *IAR3*, *ILL5*, and *ILL6* was essentially lost in the JA-insensitive mutant *coi1* (Fig. 3, A–C), and strongly attenuated for *ILL1*. This suggests a functional link between these hydrolases and the JA pathway, and extends the previous report of COI1-dependent induction of *IAR3* (29). Moderate (*ILL1*) or weak (*ILL2* and *ILL3*) constitutive expression was evidenced for other genes, with *ILL1* and *ILL2* being down-regulated, and *ILL3* unaffected by leaf wounding (data not shown). Among inducible genes, *IAR3* had the highest basal expression level in leaves and *ILL5* had the lowest (Fig. 3E), explaining the strong difference in induction factors between these genes in WT plants (Fig. 3). Furthermore, when induction factors are multiplied by basal expression, maximal expression levels appear about 20-fold lower for *ILL1* than for *IAR3*, *ILL5*, or *ILL6*. These results prompted us to focus on the impact of the

Jasmonate Conjugate Cleavage and Tuberonic Acid Formation

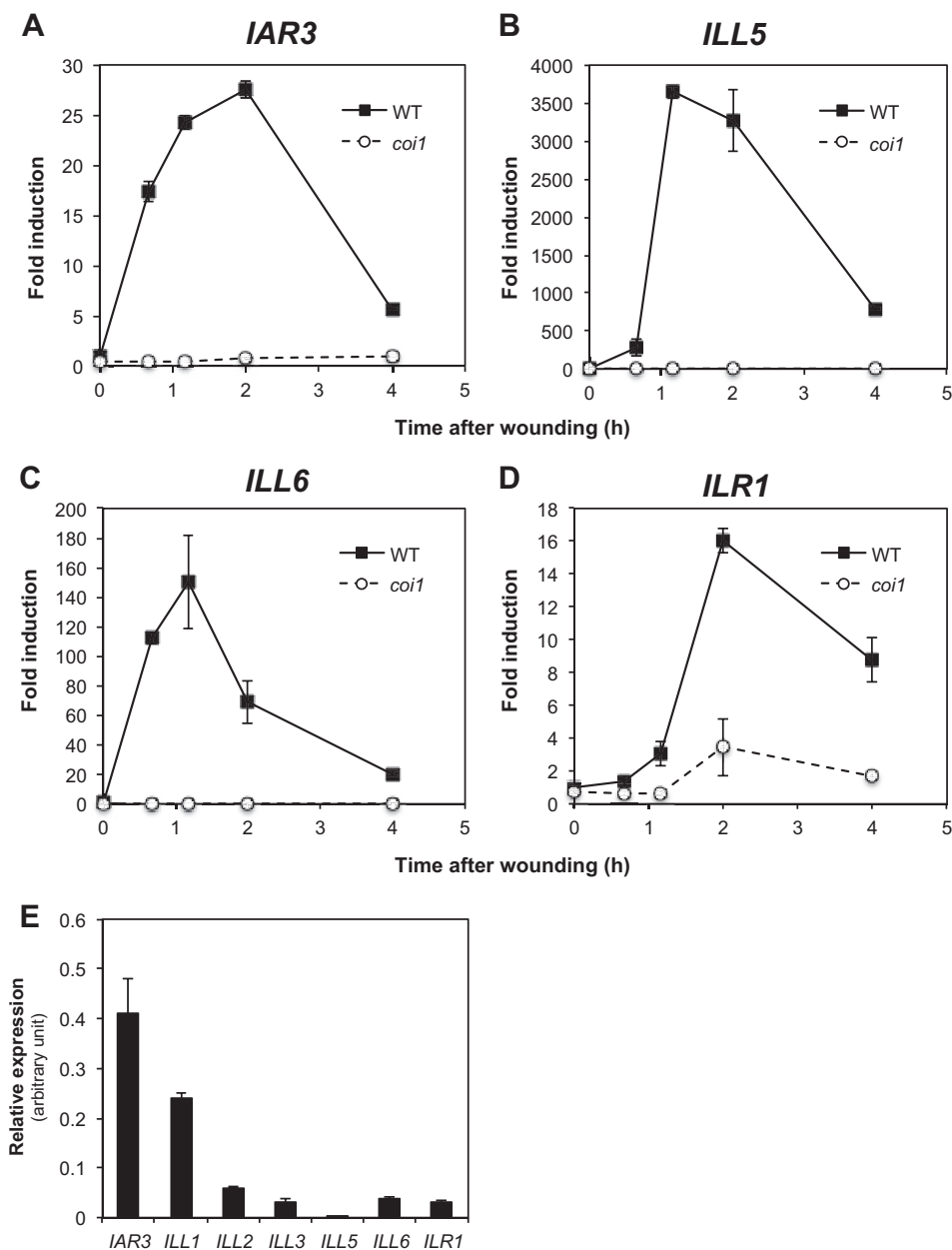


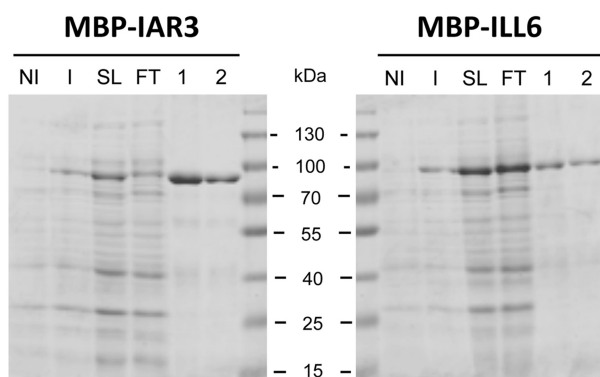
FIGURE 3. **Amidohydrolase gene expression in wounded WT and *coi1* plants.** Leaves were harvested at increasing times after wounding and submitted to RNA extraction. One μg of total RNA was reverse transcribed and expression of *IAR3* (A), *ILL5* (B), *ILL6* (C), and *ILR1* (D) was determined by real-time PCR using two reference genes. Expression is represented as fold-induction relative to the level at time 0 in WT that was set to 1 for each gene. E, relative expression of the 7 gene members of the *Arabidopsis* *ILR1* family in unstressed leaves. Triplicate determinations \pm S.E. are shown.

three wound-responsive, highly expressed amidohydrolase genes *IAR3*, *ILL5*, and *ILL6* on jasmonate metabolism.

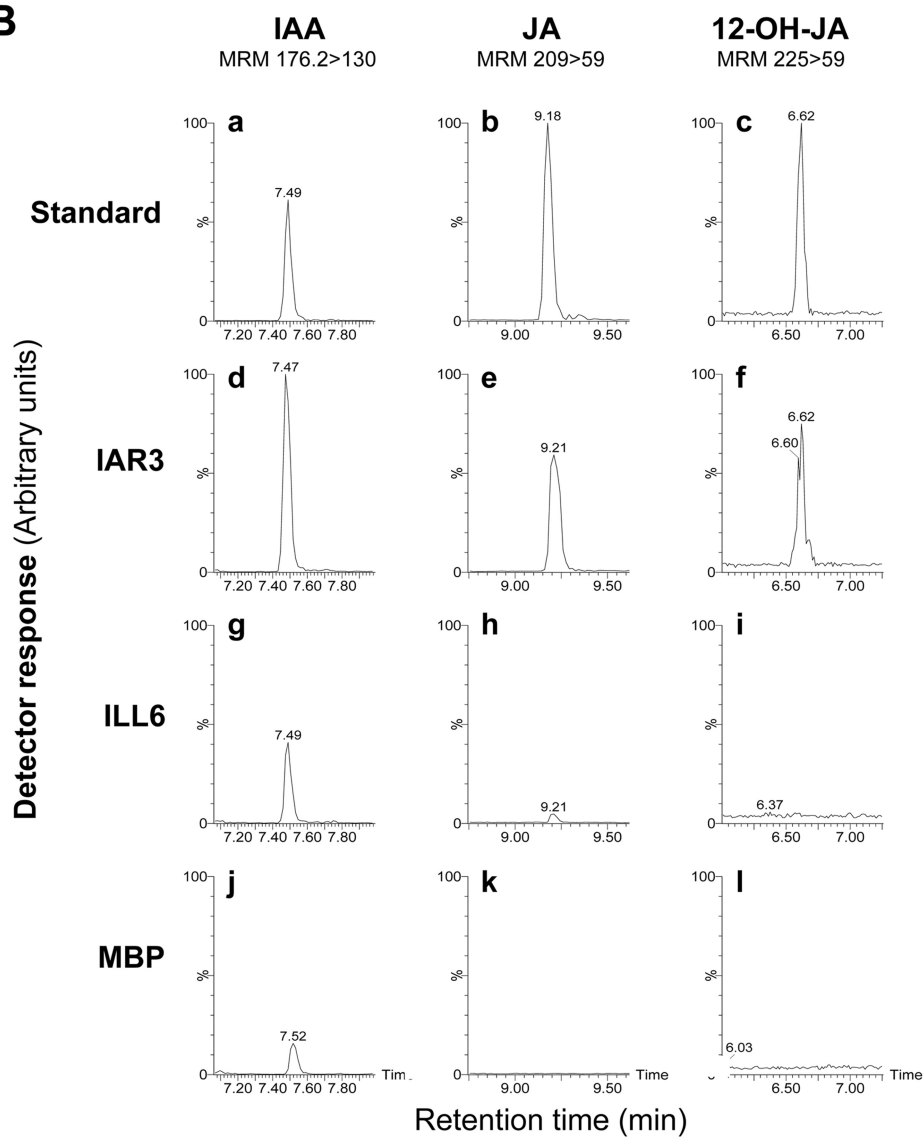
Amidohydrolase Activity of Recombinant *IAR3* and *ILL6* on JA-Ile and Oxidized Derivatives—Recombinant *IAR3*, *ILL1*, *ILR1*, and *ILL2* were described as cleaving several auxin-amino acid conjugates, with *ILL2* displaying very high activity on IAA-alanine (28, 36). Accordingly, roots from several amidohydrolase mutants displayed altered growth responses to exogenously supplied conjugates (27, 36). In contrast, no conditions were found in which glutathione *S*-transferase-*ILL6* fusions hydrolyze IAA-amino acids (36). Recently, the *IAR3*-related JIH protein, whose gene is wound- and jasmonate-induced in *N. attenuata*, was shown to cleave similarly JA-Ile and IAA-Ala *in vitro* (40). We expressed recombinant *IAR3* and *ILL6* devoid

of their N-terminal signal peptides in *E. coli* as maltose-binding protein fusions before affinity purification through their His tag (Fig. 4A). *ILL5* protein was not further studied here as its cloned cDNA was repeatedly found to bear a 7-nucleotide deletion introducing a frameshift and a premature stop codon compared with the TAIR gene model, comforting an earlier suspicion that *ILL5* may be a pseudogene (28). Purified *IAR3* and *ILL6* were incubated in parallel with synthetic JA-Ile, 12OH-JA-Ile, 12COOH-JA-Ile, and IAA-Ala, and corresponding unconjugated compounds were searched for as a measurement of cleaving activity. Fig. 4B shows typical UPLC-MS/MS chromatograms obtained with either fusion protein or maltose-binding protein as a control. Both enzymes were found to release JA from JA-Ile (Fig. 4B, e and h) and IAA from IAA-Ala (Fig. 4B, d

A



B



C

	JA-Ile	12OH-JA-Ile	12COOH-JA-Ile	IAA-Ala
IAR3	355.8 ± 52.4	38.4 ± 6.7	nd	268.7 ± 14.6
ILL6	17.0 ± 1.4	nd	nd	20.2 ± 0.76

Jasmonate Conjugate Cleavage and Tuberonic Acid Formation

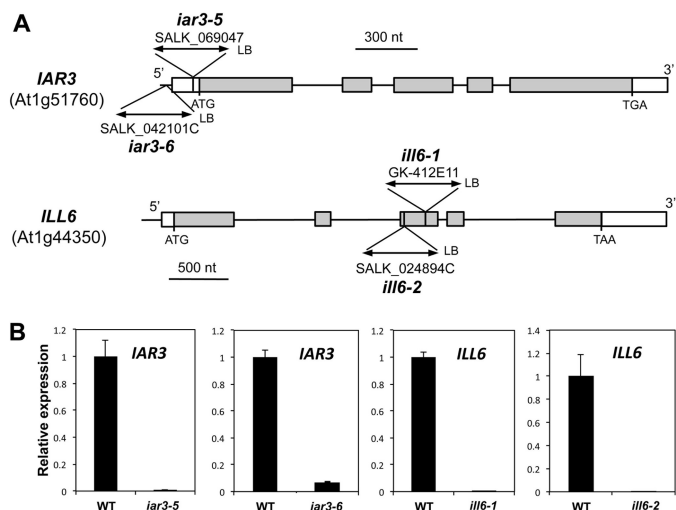


FIGURE 5. Molecular characterization of *iar3* and *ill6* insertion alleles. *A*, positions of T-DNA insertions in the different mutant lines are shown, and for each allele the position of the left border (LB) is indicated. Boxes denote exons and thin vertical lines denote introns or promoter regions. White boxes depict untranslated regions and gray boxes coding regions. *B*, RT-qPCR analysis of gene expression in WT and mutant leaves. Leaves were harvested 1 h after wounding and abundance of transcript regions spanning the insertion site was monitored. Expression in mutant lines was calculated relative to WT levels set to 1. Expression was normalized using two reference genes.

and *g*), recombinant ILL6 appearing less active than IAR3 on all compounds tested. When incubated with 12OH-JA-Ile, TA signal was detected only with IAR3 (Fig. 4*B, f*), whereas after incubation with 12COOH-JA-Ile, no cleavage activity was evidenced with either enzyme (data not shown). The different activities were evaluated quantitatively after establishing standard curves with pure compounds. Under the conditions used IAR3 was about 20-fold more active on JA-Ile than ILL6, and IAR3 was itself 9-fold more active on JA-Ile than on 12OH-JA-Ile (Fig. 4*C*). These results from *in vitro* experiments show that IAR3 and ILL6 release JA from JA-Ile and that at least IAR3 can also generate TA by cleaving 12OH-JA-Ile.

Amidohydrolase Mutants Display Elevated Oxidized JA-Ile Conjugates and Reduced TA Levels—To obtain direct genetic evidence for amidohydrolase involvement in jasmonate metabolism during the wound response, we used T-DNA insertion mutant lines that are impaired in the expression of *IAR3* and *ILL6*. The EMS alleles *iar3-1* through *iar3-4* were previously described (28), therefore we named the T-DNA alleles used here *iar3-5* and *iar3-6* (Fig. 5*A*). No *ill6* alleles were previously reported, and we introduce in this study *ill6-1* and *ill6-2*. All alleles were found to have undetectable transcript levels, except *iar3-6*, which had an insertion in the promoter region and appeared as a strong knock-down allele (Fig. 5*B*). The wound-induced content in five JAs of *iar3-5*, *ill6-1*, and *iar3-6*, *ill6-2* plants was determined relative to WT in two independent

series of kinetic experiments. As shown in Fig. 6*A*, JA-Ile was found similar to WT levels, except in *iar3-5* that showed increased levels at early time points, a result that is consistent with the respective *in vitro* JA-Ile cleaving activities found for IAR3 and ILL6. Mutations had little impact on JA levels that fluctuated near WT levels in the different alleles (Fig. 6*B*). We next examined the profiles of oxidized jasmonates. 12OH-JA-Ile was significantly hyperaccumulated in *ill6* and in *iar3* mutants (Fig. 6*C*), and this increase was accompanied by a corresponding reduction in 12OH-JA (TA) levels in all examined alleles (Fig. 6*D*). By 4 h post-wounding, amidohydrolase mutants accumulated about 50–60% WT TA levels. Finally, we quantified 12COOH-JA-Ile levels *in planta*, the second oxidation product, generated mainly by CYP94C1 (20). This required its prior chemical synthesis that is extensively described under [supplemental Methods S1](#) as an original method. We determined that 12COOH-JA-Ile accumulated abundantly to about 10–25 nmol/g of fresh weight by 4 h post-wounding (Fig. 6*E*), making it a highly abundant jasmonate in wounded *Arabidopsis* leaves. Its levels were further enhanced in amidohydrolase mutants relative to WT, particularly in *iar3-5* and *ill6-1*. The overall differences in levels of metabolites, especially of Ile conjugates, in the two independent experiments (Fig. 6, *left versus right panels*) may illustrate adaptation of jasmonate dynamics to different growth periods or slight changes in experimental setup. The milder chemotypes recorded for all compounds in *iar3-6* are consistent with this line being a weaker allele than *iar3-5* (Fig. 5*B*). The simplest interpretation of these genetic data are that similarly to JIH in *N. attenuata* (40), IAR3 and ILL6 readily hydrolyze JA-Ile *in vivo* and the two *Arabidopsis* enzymes likely also act on 12OH-JA-Ile. Consequently, they establish that a significant part of the TA accumulated in response to wounding is generated via the cleavage of 12OH-JA-Ile.

TA, one of the products of amidohydrolase activity, is also known to undergo further metabolism via two competing routes (2), one leading to the TA glucoside (TA-Glc), the other yielding the sulfonated derivative 12-HSO₄-JA (13, 14). We therefore investigated if differential TA conversion could result in variable TA levels in the different mutant backgrounds. Transcripts of *ST2a*, the gene encoding the TA-sulfotransferase (13), were strongly up-regulated in wounded leaves in a *coi1*-dependent manner (Fig. 7*A*), whereas this induction was similar to WT in *jar1* (Fig. 7*B*) or in *iar3-6* or *ill6-2* mutants (Fig. 7*C*). Therefore, consumption of TA substrate by *ST2a* is not predicted to be affected differentially in these latter lines. Direct measurement of 12-HSO₄-JA established the rather late wound accumulation of this compound, and its relative abundance was reduced by about 60% in *jar1* and 40% in amidohy-

FIGURE 4. Purification and enzymatic activity of recombinant IAR3 and ILL6 amidohydrolases. *A*, purification steps were analyzed by 12.5% SDS-PAGE. Total proteins from bacteria transformed with plasmids expressing fusion proteins were analyzed before (non-induced, NI) and after (induced, I) induction with 0.5 mM isopropyl 1-thio- β -D-galactopyranoside for 4 h. Fusion proteins are visible after induction. His-tagged proteins present in soluble lysate (SL) were purified by affinity chromatography. FT, flow through. 1 and 2, elution fractions 1 and 2. Molecular mass markers are indicated. Proteins were visualized by Coomassie staining. *B*, 20 μ g of either protein were incubated with the following amino acid conjugates as candidate substrates: IAA-Ala, JA-Ile, and 12OH-JA-Ile. LC chromatograms are shown where the cleavage products IAA (panels *a, d, g, and j*), JA (panels *b, e, h, and k*), or 12OH-JA (panels *c, f, i, and l*) were separated by UPLC-MS/MS and detected by their indicated multiple reaction monitoring transitions. *C*, specific activities (pmol/h/mg of protein) were determined by incubation of purified enzymes for 90 min with 100 μ M substrates and quantification of cleavage products with authentic standards curves. Values represent mean \pm S.E. ($n = 3$). nd, not detected.

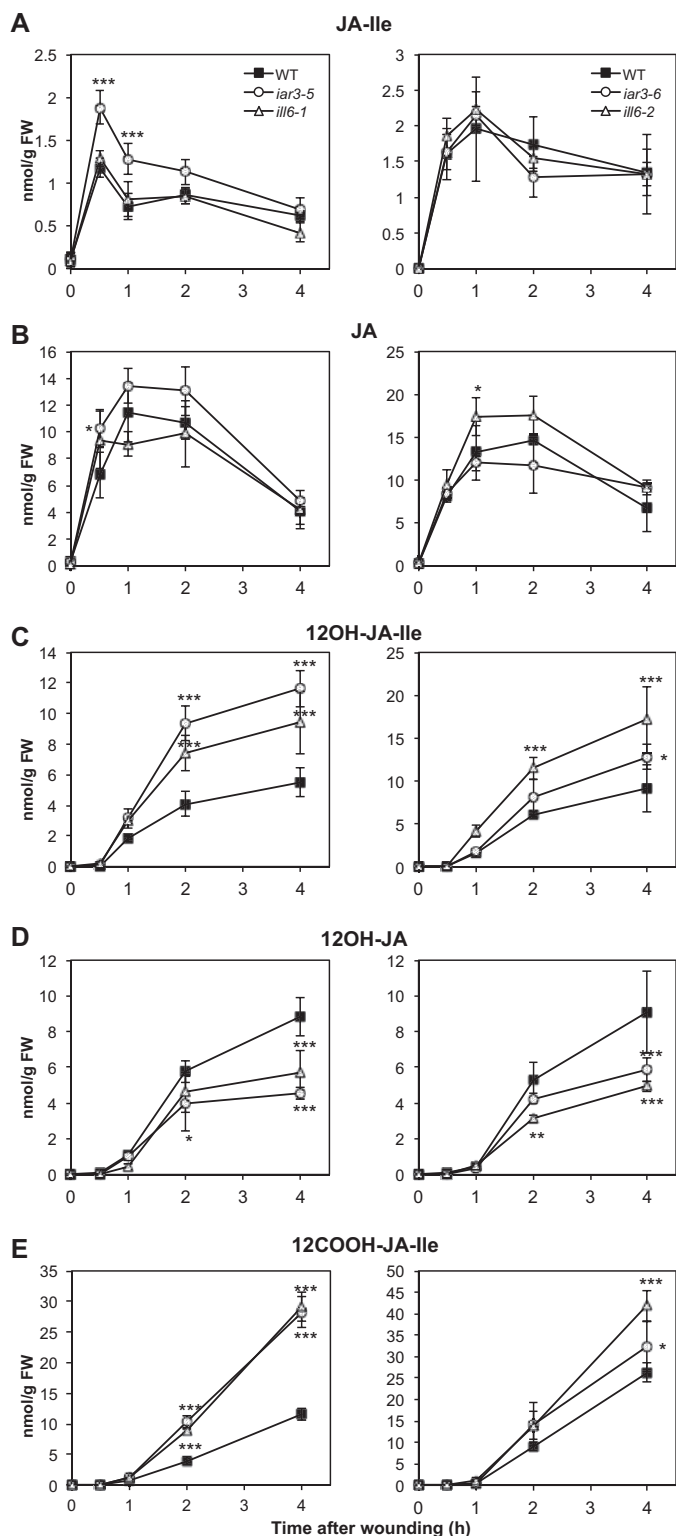


FIGURE 6. Kinetic analysis of jasmonate accumulation in wild-type (WT) and in *iar3* and *ill6* mutant plants upon leaf wounding. *iar3-5* with *ill6-1* and *iar3-6* with *ill6-2* lines were analyzed along with WT plants in independent experiments. Leaves were harvested at increasing times after wounding and extracted for jasmonate determination by UPLC-MS/MS. A, JA-Ile; B, JA; C, 12OH-JA-Ile; D, 12OH-JA; E, 12COOH-JA-Ile. Data are mean \pm S.E. from three biological samples. Asterisks indicate significant differences between mutant and WT at $p < 0.05$ (*), $p < 0.01$ (**) or $p < 0.001$ (***) (two-way ANOVA).

drolase mutants by 4 h (Fig. 7D). No TA-specific glucosyltransferase is characterized in *Arabidopsis*, but such an activity has been described in rice (41). We found that TA-Glc accumulation was strongly impaired in *jar1* and significantly reduced in *iar3-6* or *ill6-2* mutants (Fig. 7E). Collectively, these results suggest that the two known TA conversion pathways are not enhanced in *iar3-6* or *ill6-2* and that reduced TA accumulation is mostly due to impaired hydrolytic activity. In addition, they provide evidence that 12-HSO₄-JA and TA-Glc partly derive from TA generated through the deconjugation pathway uncovered in this work.

JA-Ile Turnover Is Tightly Controlled by Compensating Oxidative and Hydrolytic Catabolic Pathways—The observation that JA-Ile levels are only moderately or not altered by mutations in amidohydrolase genes (Fig. 6A), is in contrast to the hyperaccumulation of its two oxidized derivatives (Fig. 6, C and E) and may be indicative of enhanced hormone turnover in these lines. To examine this possibility, we monitored by RT-qPCR the wound-induced expression of genes encoding known JA-Ile-metabolizing enzymes, either from the *CYP94* family or the respective non-mutated amidohydrolase gene. Fig. 8A shows that in either *ill6* allele, *IAR3* transcript levels significantly exceeded those in WT at 1 h post-wounding. In contrast, *ILL6* expression was only marginally affected by *IAR3* deficiency (Fig. 8B). In addition, *CYP94B3* transcripts, encoding the primary enzyme for oxidative JA-Ile inactivation (20–22) were found hyperaccumulated in both *ill6* alleles, but not in *iar3* alleles (Fig. 8D). *CYP94B1*, that also catalyzes JA-Ile hydroxylation *in vitro*,⁴ showed more variable transcript levels between mutants (Fig. 8C). *CYP94C1* catalyzes the second JA-Ile oxidation step (20), and was hyperinduced in all four alleles (Fig. 8E), consistent with a pronounced 12COOH-JA-Ile overaccumulation in these mutants (Fig. 6E). This expression survey points to the existence of compensation mechanisms (mainly when *ILL6* is impaired) where the reduced JA-Ile-cleaving activity results in a stronger or earlier up-regulation of the other genes encoding JA-Ile-consuming enzymes to prevent an excessive accumulation of the hormone. Conversely, the weaker reciprocal compensation in *iar3-5* correlated with higher impacts of *IAR3* deficiency on JA-Ile levels (Fig. 6A). We finally checked if *cyp94* mutants exhibited a similar compensation by the amidohydrolase pathway. The expression patterns of *IAR3* and *ILL6* in *cyp94b3* and *cyp94b3c1* were similar to WT (data not shown), in good agreement with the highly persistent JA-Ile accumulation that was described previously in these lines (20, 22).

DISCUSSION

Plant hormone inactivation and turnover generally proceeds through two major pathways. The first route leads to sugar or amino acid conjugates and has been mostly studied for auxin (42), but was also reported for other hormones. The second pathway operates through oxidations typically catalyzed by CYP enzymes belonging to distinct subfamilies (23). Amide conjugates are synthesized by the so-called GH3 family and in the case of auxin their formation is believed to ensure removal or storage of excessive free active hormone (43). This conjuga-

⁴ E. Widemann and F. Pinot, unpublished data.

Jasmonate Conjugate Cleavage and Tuberonic Acid Formation

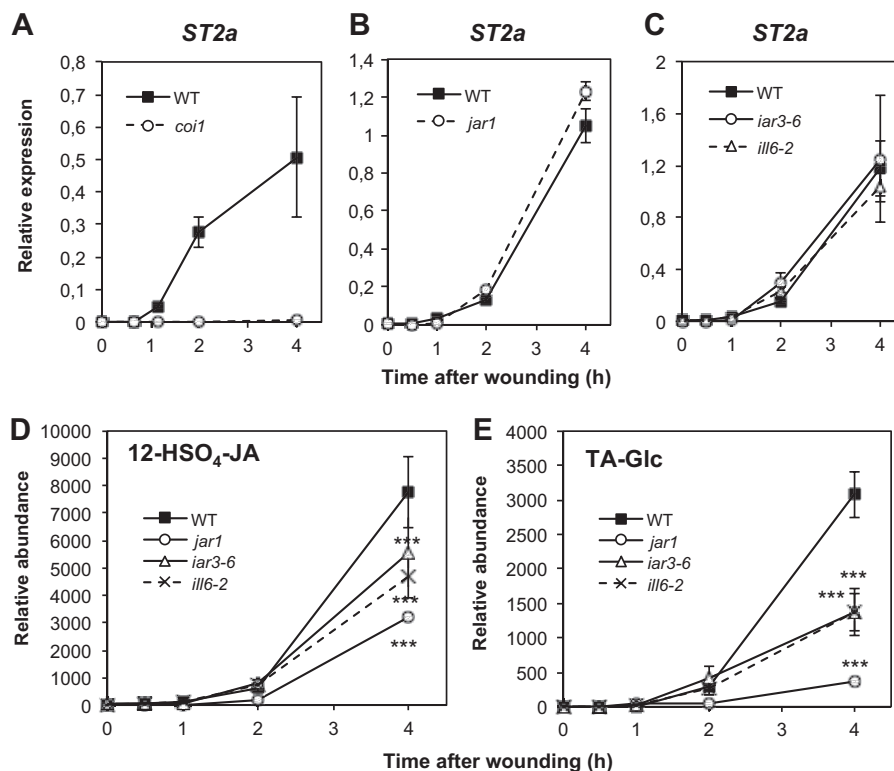


FIGURE 7. Analysis of tuberonic acid metabolism pathways in *jar1*, *coi1*, and amidohydrolase mutants upon wounding. Leaves were harvested at increasing times after wounding and submitted to RNA extraction. Expression of *ST2a* was examined by real-time PCR in *coi1* (A), *jar1* (B), and *iar3-6* and *ill6-2* (C) mutants relative to WT and represented as $\Delta\Delta C_t$ values. Two reference genes were used for normalization. The TA derivatives 12-HSO₄-JA (D) and tuberonic acid glucoside (TA-Glc, E) levels were determined in WT, *jar1*, *iar3-6*, and *ill6-2* plants. Triplicate determinations \pm S.E. are shown for all analyses. Asterisks indicate significant differences between mutant and WT at $p < 0.001$ (two-way ANOVA).

tion is reversible as several members of the ILR1-like family of amidohydrolases release free auxin from such compounds (36).

The case of jasmonate is a remarkable exception to this scheme as conjugation of JA to Ile by JAR1 (GH3.11) is the critical hormone activation step. We and others have characterized recently a CYP94-based JA-Ile catabolic pathway that generates hydroxylated and carboxylated JA-Ile derivatives and contributes largely to the rapid hormone clearance after leaf wounding (20–22). Unconjugated jasmonates also occur as oxidized derivatives, namely tuberonic acid (2, 13, 14, 41). Despite its abundance in several plant species, the question of the mode of TA formation has remained unsolved, as no enzyme for direct hydroxylation of JA could be characterized. We have provided in this work biochemical and genetic evidence that JA-Ile catabolism and TA formation are linked through the action of two amidohydrolases. Although the family of ILR1-like (ILL) amidohydrolases was discovered in the context of auxin metabolism (42, 44), a closer examination revealed that *IAR3*, *ILL5*, and *ILL6* genes are strongly co-regulated with the JA metabolic and signaling pathway. Consistently, we demonstrated their rapid and COI1-dependent up-regulation upon wounding, with kinetics similar to the oxidative branch of JA-Ile catabolism represented by the *CYP94B3* and *CYP94C1* genes (20). *ILL1*, despite a lower expression level, also displays COI1-dependent wound induction, and must be analyzed in the context of jasmonate metabolism. Based on their transcriptional behavior and abundant expression, *IAR3* and *ILL6* were the prime candidates for a role in jasmonate metabolism,

whereas *ILL5* is a non-coding sequence, and *ILL1*, *ILL2*, and *ILL3* transcripts do not correlate with jasmonate conjugate abundance. Similarly to the recently described related JIH enzyme in *N. attenuata* (40), recombinant IAR3 and ILL6 hydrolyzed almost equally JA-Ile and IAA-Ala, and IAR3 was also found to act on the oxidized derivative 12OH-JA-Ile. IAR3 was previously shown to cleave abscisic acid amino acid conjugates *in vitro* (45) and appears to be a versatile enzyme, but actual catalysis may be determined *in vivo* by substrate abundance. *In vitro* activity of recombinant ILL6 was much lower than IAR3 on either JA-Ile or IAA-Ala and no activity could be detected on 12OH-JA-Ile under our assay conditions. Previous attempts to produce active AtILL6 (36) or the *Brassica* homolog BrILL6 (25) in bacteria have failed, one possible reason being the presence of potential transmembrane domain(s). These limitations leave open the possibility that the *in vitro* enzymatic data presented here have under evaluated the catalytic capacities of AtILL6.

Genetic analysis has provided novel insights into the impact of IAR3 and ILL6 in metabolism of jasmonate conjugates in *Arabidopsis*. Although JA-Ile appeared as the best *in vitro* substrate tested, IAR3 or ILL6 deficiency had little apparent impact on the accumulation of the hormone, in contrast to JIH-silenced *N. attenuata* plants (40). This observation points to JA-Ile as a central component in the JA pathway, not only by its hormonal activity, but also as a metabolic hub with links to other conjugated and non-conjugated jasmonates. We established that the increased JA-Ile accumulation expected from

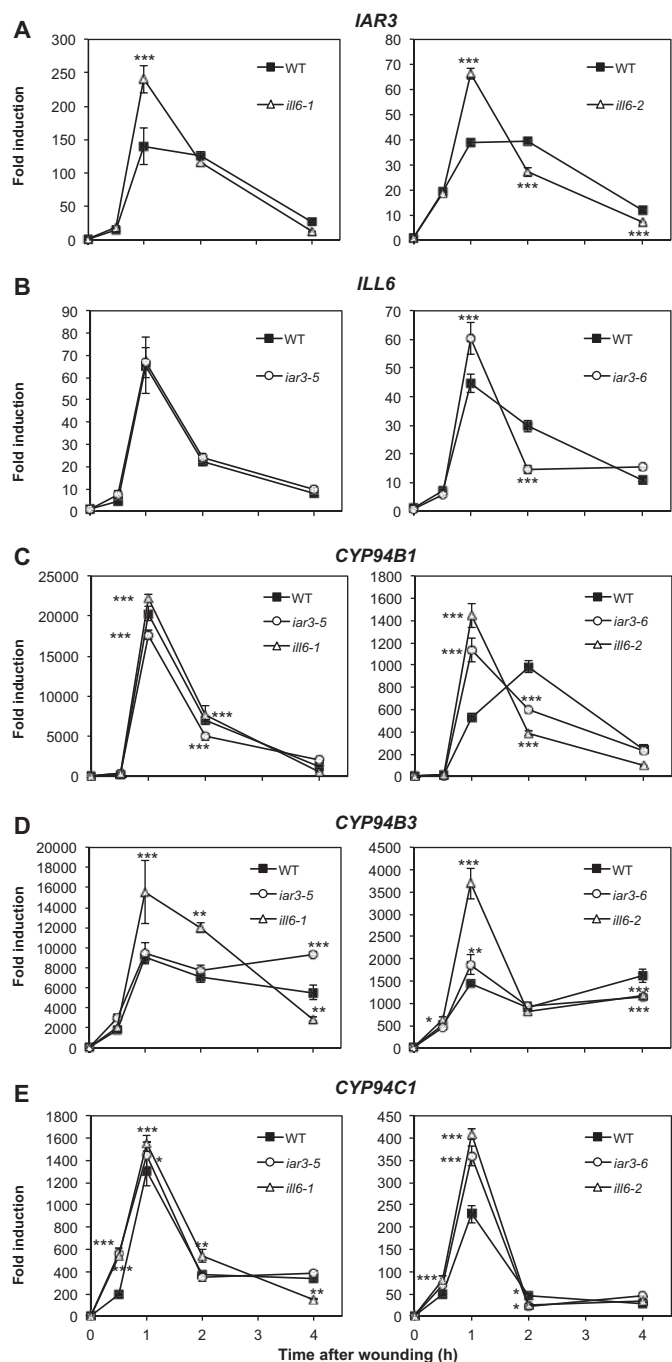


FIGURE 8. Impact of amidohydrolase mutations on expression of genes encoding JA-Ile metabolizing enzymes. Total RNA was extracted from wounded plants analyzed kinetically for jasmonate content in Fig. 6 and reverse-transcribed. Gene expression time courses were established for the following genes by real-time PCR: A, *IAR3*; B, *ILL6*; C, *CYP94B1*; D, *CYP94B3*; and E, *CYP94C1*. Expression is represented as fold-induction relative to level at time 0 in WT plants, which was set to 1 for each gene. Differences between the left and right panel fold-inductions are due to differences in basal expression levels between independent batches of plants. Two reference genes were used for normalization. Triplicate determinations \pm S.E. are shown. Asterisks indicate significant differences between mutant and WT at $p < 0.05$ (*), $p < 0.01$ (**), or $p < 0.001$ (***) (two-way ANOVA).

reduced amidohydrolase activity is likely counterbalanced by a stronger induction of other genes encoding JA-Ile-consuming enzymes, such as *IAR3* and *CYP94B3* and *CYP94C1* transcripts in *ill6* alleles. In contrast, in the *iar3-5* allele, such a transcrip-

tional compensation was not evidenced, and accordingly, this line accumulated more JA-Ile than WT. Conversely, it is worth noting that the higher and persistent JA-Ile hyperaccumulation in *cyp94b3* and *cyp94b3c1* mutants blocked in oxidative JA-Ile catabolism (20) was not associated with hyperinduction of amidohydrolase genes. When manipulating *Arabidopsis* plants genetically to increase or stabilize JA-Ile levels, selective compensation can occur by enhanced stimulation of other enzymes catabolizing JA-Ile. This flexible response illustrates the metabolic plasticity of the JA pathway to maintain proper regulation of active hormone levels. JA-Ile dynamics are under high flux through both oxidation and cleavage pathways that prevent excessively high levels to build up. Consequently, if metabolic control of JA signaling is determined solely by JA-Ile levels, one may anticipate little impact of amidohydrolase deficiency on physiological JA responses. Also, the exact extent of functional redundancy between *IAR3* and *ILL6*, as well as the role of *ILR1*, needs to be investigated by combining mutations.

A close examination of metabolic profiles in different JA pathway mutants led us to the first description of a metabolic route leading to the abundant jasmonate TA. Several lines of genetic evidence indicate that TA accumulation is achieved by a route that is dependent on JA conjugation, oxidation, and cleavage. First, the *jar1* mutation lowers by more than half the TA content compared with WT. The remaining TA accumulating in *jar1* may arise through a *JAR1*-independent route, for example, by cleaving other oxidized JA-amino acid conjugates generated by distinct GH3 enzymes, but such conjugate pools seem quantitatively minor in wounded *Arabidopsis* leaves (46) to account for the significant levels of TA in *jar1*. Alternatively, the *jar1*-independent TA pool may reflect the existence of a direct JA-hydroxylation route by still unknown hydroxylase(s). Under our conditions, none of the 6 recombinant *Arabidopsis* CYP94 proteins showed JA-hydroxylase activity.⁴ Second, mutants in *cyp94* genes that govern JA-Ile oxidation displayed reduced TA levels despite of abundant JA supply similarly to *jar1*, questioning the importance of direct hydroxylation for TA formation. The higher abundance of TA in *cyp94b3c1* than in *cyp94c1* is well correlated with more 12OH-JA-Ile being available in the double mutant because of impaired 12COOH-JA-Ile formation (Fig. 2). Third, depleting either *IAR3* or *ILL6* amidohydrolase resulted in hyperaccumulation of 12OH-JA-Ile with a concomitant reduction in TA levels (Fig. 6), pointing to a direct substrate-product link between these two JAs. The analysis of two known TA modification routes confirmed that TA itself is a metabolic intermediate. Abundance of both 12-HSO₄-JA and TA-Glc was correlated with TA levels in the different genetic backgrounds. This characteristic makes them direct TA derivatives and extends the number of JAs whose formation requires a conjugation-oxidation-deconjugation cascade.

The impact of amidohydrolase inactivation was much stronger on the two oxidized conjugates than on JA-Ile. As discussed above, an excess of uncleaved JA-Ile or 12OH-JA-Ile can alternatively be cleared by enhanced CYP94-mediated oxidation that shifts the pool of jasmonates toward more oxidized conjugates. The fate of the long-lived 12COOH-JA-Ile is the less well known. We have described its first chemical synthesis that

Jasmonate Conjugate Cleavage and Tuberonic Acid Formation

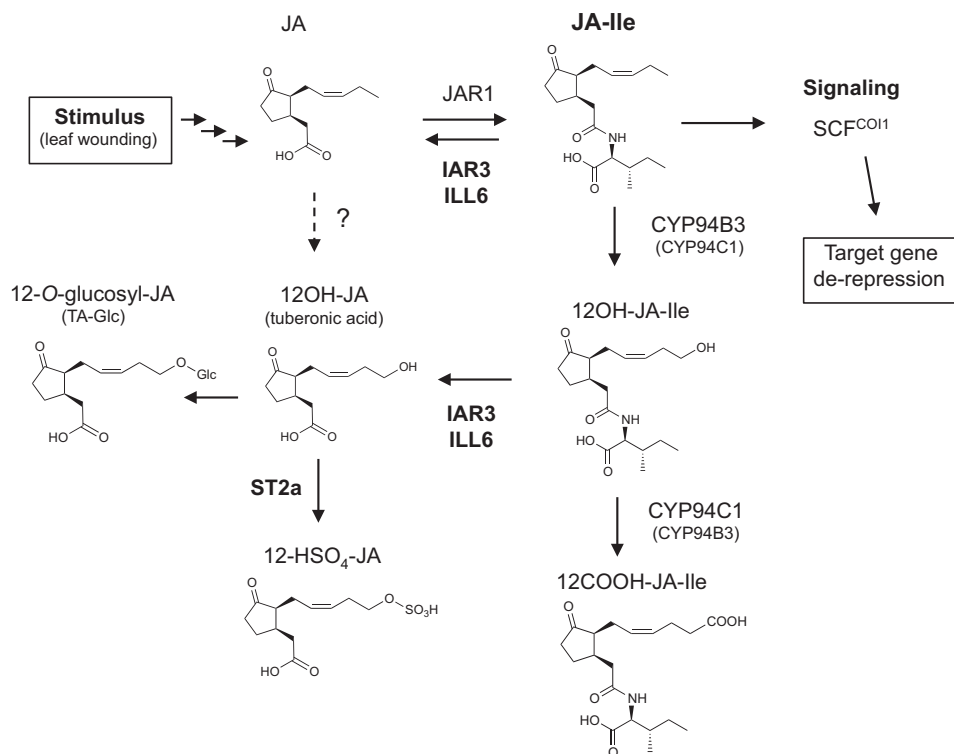


FIGURE 9. **Proposed model for interconversion routes between JA and its oxidized and/or Ile-conjugated derivatives in *Arabidopsis*.** Upon stimulation following leaf wounding, JA biosynthesis is strongly activated, including further metabolism to an array of derivatives. Part of JA is conjugated to isoleucine, forming JA-Ile that is transiently accumulated as the active hormonal signal. JA-Ile is rapidly inactivated/eliminated by two simultaneously up-regulated COI1-dependent enzymatic pathways, one that is CYP94-based and leads to oxidized derivatives, and the second by conjugate cleavage under the action of the amidohydrolases IAR3 and ILL6. The compounds are shown in the demonstrated (up to JA-Ile) or supposed (3,7)-*cis* stereochemistry occurring *in planta*.

allowed its quantification, and revealed high levels in plant extracts. No cleavage of 12COOH-JA-Ile has been evidenced. Precise analysis of potential *in vitro* and *in planta* cleavage of this compound awaits the availability of synthetic 12COOH-JA. In any case, as the most downstream JA-Ile catabolite, largely enhanced 12COOH-JA-Ile levels in *iar3* and *ill6* mutants result from the cumulative effects of uncleaved JA-Ile and 12OH-JA-Ile that are available for oxidation.

Collectively, the mutant analysis along with partial *in vitro* enzymatic data establish an original and indirect metabolic route to TA formation that requires the sequential conjugation, oxidation, and cleavage of JA. It also reveals that part of the wound-induced TA accumulates in *Arabidopsis* as a by-product of JA-Ile turnover rather than a JA shunt upstream of hormone activation. Our study proposes a novel function for IAR3 in jasmonate metabolism and describes the first functional data for ILL6, both enzymes reversing the action of JAR1. Whereas previous IAR3 impact on metabolism was evidenced after supplying exogenous auxin conjugates (28, 36) to *Arabidopsis* seedlings, the data presented here show the impact of its activity on endogenously generated substrates.

In summary, the transient nature of the JA-Ile burst triggered by wounding is shaped by the rapid, simultaneous and COI1-dependent up-regulation of two hormone inactivation pathways (Fig. 9): the first route is contributed by the CYP94-based oxidation to 12OH-JA-Ile and 12COOH-JA-Ile (20–22); the second pathway examined in this study is represented by the IAR3 and ILL6 amidohydrolases that proceed to the cleavage of JA-Ile and the 12OH-JA-Ile oxidized conjugate. The fact that JA

pathway activation triggers both conjugation and deconjugation steps to form and eliminate the active hormone is intriguing. It is not known if JA issued from deconjugation is recycled for further JA-Ile signaling or if it engages into an independent metabolic route. The combined action of both oxidative and hydrolytic pathways identifies an additional metabolic function by producing a significant part of wound-induced TA and TA derivatives. The availability of these novel genetic backgrounds impaired in jasmonate metabolism will allow deeper exploration of the complex regulation of JA-Ile hormone homeostasis.

Acknowledgments—We are grateful to Dr. Rozenn Ménard for critical reading of the manuscript and Dr. Nicolas Baumberger for help in recombinant protein production. We thank the gardener team for producing the numerous plants used in this study, and the Nottingham *Arabidopsis* Stock Center for providing seeds of T-DNA insertion lines. The UPLC-MS/MS instrument was co-financed by the Centre National de la Recherche Scientifique, the Université de Strasbourg, the Région Alsace, the Institut National de la Recherche Agronomique, and the Tepral Company.

Addendum—During the review of this paper, a paper was published (47) that partially describes *ill6* insertion mutants. The *ill6-1* line used in Ref. 47 corresponds to the *ill6-2* allele analyzed in the present study.

REFERENCES

- Browse, J. (2009) Jasmonate passes muster. A receptor and targets for the defense hormone. *Annu. Rev. Plant Biol.* **60**, 183–205
- Wasternack, C., and Hause, B. (2013) Jasmonates. Biosynthesis, percep-

- tion, signal transduction and action in plant stress response, growth and development. *Ann. Bot.* **111**, 1021–1058
3. Erb, M., Meldau, S., and Howe, G. A. (2012) Role of phytohormones in insect-specific plant reactions. *Trends Plant Sci.* **17**, 250–259
 4. Koo, A. J., and Howe, G. A. (2009) The wound hormone jasmonate. *Phytochemistry* **70**, 1571–1580
 5. Verhage, A., Vlaardingbroek, I., Raaymakers, C., Van Dam, N. M., Dicke, M., Van Wees, S. C., and Pieterse, C. M. (2011) Rewiring of the jasmonate signaling pathway in *Arabidopsis* during insect herbivory. *Front. Plant Sci.* **2**, 47
 6. Mithöfer, A., and Boland, W. (2012) Plant defense against herbivores. Chemical aspects. *Annu. Rev. Plant Biol.* **63**, 431–450
 7. Wu, J., and Baldwin, I. T. (2010) New insights into plant responses to the attack from insect herbivores. *Annu. Rev. Genet.* **44**, 1–24
 8. Glauser, G., Grata, E., Dubugnon, L., Rudaz, S., Farmer, E. E., and Wolfender, J. L. (2008) Spatial and temporal dynamics of jasmonate synthesis and accumulation in *Arabidopsis* in response to wounding. *J. Biol. Chem.* **283**, 16400–16407
 9. Glauser, G., and Wolfender, J. L. (2013) A non-targeted approach for extended liquid chromatography-mass spectrometry profiling of free and esterified jasmonates after wounding. *Methods Mol. Biol.* **1011**, 123–134
 10. Chung, H. S., Koo, A. J., Gao, X., Jayanty, S., Thines, B., Jones, A. D., and Howe, G. A. (2008) Regulation and function of *Arabidopsis* JASMONATE ZIM-domain genes in response to wounding and herbivory. *Plant Physiol.* **146**, 952–964
 11. Koo, A. J., and Howe, G. A. (2012) Catabolism and deactivation of the lipid-derived hormone jasmonoyl-isoleucine. *Front. Plant Sci.* **3**, 19
 12. Yoshihara, T., Omer, E.-L. A., Koshino, H., Sakamura, S., Kikuta, Y., and Koda, Y. (1989) Structure of a tuber-inducing stimulus from potato leaves (*Solanum tuberosum* L.). *Agric. Biol. Chem.* **53**, 2835–2837
 13. Gidda, S. K., Miersch, O., Levitin, A., Schmidt, J., Wasternack, C., and Varin, L. (2003) Biochemical and molecular characterization of a hydroxy-jasmonate sulfotransferase from *Arabidopsis thaliana*. *J. Biol. Chem.* **278**, 17895–17900
 14. Miersch, O., Neumerkel, J., Dippe, M., Stenzel, I., and Wasternack, C. (2008) Hydroxylated jasmonates are commonly occurring metabolites of jasmonic acid and contribute to a partial switch-off in jasmonate signaling. *New Phytol.* **177**, 114–127
 15. Nakamura, Y., Mithöfer, A., Kombrink, E., Boland, W., Hamamoto, S., Uozumi, N., Tohma, K., and Ueda, M. (2011) 12-Hydroxyjasmonic acid glucoside is a COI1-JAZ-independent activator of leaf-closing movement in *Samanea saman*. *Plant Physiol.* **155**, 1226–1236
 16. Staswick, P. E., and Tiryaki, I. (2004) The oxylipin signal jasmonic acid is activated by an enzyme that conjugates it to isoleucine in *Arabidopsis*. *Plant Cell* **16**, 2117–2127
 17. Staswick, P. E., Serban, B., Rowe, M., Tiryaki, I., Maldonado, M. T., Maldonado, M. C., and Suza, W. (2005) Characterization of an *Arabidopsis* enzyme family that conjugates amino acids to indole-3-acetic acid. *Plant Cell* **17**, 616–627
 18. Fonseca, S., Chico, J. M., and Solano, R. (2009) The jasmonate pathway. The ligand, the receptor and the core signalling module. *Curr. Opin. Plant Biol.* **12**, 539–547
 19. Katsir, L., Chung, H. S., Koo, A. J., and Howe, G. A. (2008) Jasmonate signaling. A conserved mechanism of hormone sensing. *Curr. Opin. Plant Biol.* **11**, 428–435
 20. Heitz, T., Widemann, E., Lugan, R., Miesch, L., Ullmann, P., Désaubry, L., Holder, E., Grausem, B., Kandel, S., Miesch, M., Werck-Reichhart, D., and Pinot, F. (2012) Cytochromes P450 CYP94C1 and CYP94B3 catalyze two successive oxidation steps of plant hormone jasmonoyl-isoleucine for catabolic turnover. *J. Biol. Chem.* **287**, 6296–6306
 21. Kitaoka, N., Matsubara, T., Sato, M., Takahashi, K., Wakuta, S., Kawaide, H., Matsui, H., Nabeta, K., and Matsuura, H. (2011) *Arabidopsis* CYP94B3 encodes jasmonoyl-L-isoleucine 12-hydroxylase, a key enzyme in the oxidative catabolism of jasmonate. *Plant Cell. Physiol.* **52**, 1757–1765
 22. Koo, A. J., Cooke, T. F., and Howe, G. A. (2011) Cytochrome P450 CYP94B3 mediates catabolism and inactivation of the plant hormone jasmonoyl-L-isoleucine. *Proc. Natl. Acad. Sci. U.S.A.* **108**, 9298–9303
 23. Mizutani, M., and Ohta, D. (2010) Diversification of P450 genes during land plant evolution. *Annu. Rev. Plant Biol.* **61**, 291–315
 24. Piotrowska, A., and Bajguz, A. (2011) Conjugates of abscisic acid, brassinosteroids, ethylene, gibberellins, and jasmonates. *Phytochemistry* **72**, 2097–2112
 25. Schuller, A., and Ludwig-Müller, J. (2006) A family of auxin conjugate hydrolases from *Brassica rapa*. Characterization and expression during clubroot disease. *New Phytol.* **171**, 145–157
 26. Campanella, J. J., Smith, S. M., Leib, D., Wexler, S., and Ludwig-Müller, J. (2008) The auxin conjugate hydrolase family of *Medicago truncatula* and their expression during the interaction with two symbionts. *J. Plant Growth Regul.* **27**, 26–38
 27. Rampey, R. A., LeClere, S., Kowalczyk, M., Ljung, K., Sandberg, G., and Bartel, B. (2004) A family of auxin-conjugate hydrolases that contributes to free indole-3-acetic acid levels during *Arabidopsis* germination. *Plant Physiol.* **135**, 978–988
 28. Davies, R. T., Goetz, D. H., Lasswell, J., Anderson, M. N., and Bartel, B. (1999) IAR3 encodes an auxin conjugate hydrolase from *Arabidopsis*. *Plant Cell* **11**, 365–376
 29. Titarenko, E., Rojo, E., León, J., and Sánchez-Serrano, J. J. (1997) Jasmonic acid-dependent and -independent signaling pathways control wound-induced gene activation in *Arabidopsis thaliana*. *Plant Physiol.* **115**, 817–826
 30. Berr, A., McCallum, E. J., Alioua, A., Heintz, D., Heitz, T., and Shen, W. H. (2010) *Arabidopsis* histone methyltransferase SET DOMAIN GROUP8 mediates induction of the jasmonate/ethylene pathway genes in plant defense response to necrotrophic fungi. *Plant Physiol.* **154**, 1403–1414
 31. Birkenbihl, R. P., Diezel, C., and Somssich, I. E. (2012) *Arabidopsis* WRKY33 is a key transcriptional regulator of hormonal and metabolic responses toward *Botrytis cinerea* infection. *Plant Physiol.* **159**, 266–285
 32. Kramell, T., Schmidt, J., Schneider, G., Sembdner, G., and Schreiber, K. (1988) Synthesis of *n*-(jasmonoyl)amino acid conjugates. *Tetrahedron* **44**, 5791–5807
 33. Matsuura, H., Ohmori, F., Kobayashi, M., Sakurai, A., and Yoshihara, T. (2000) Qualitative and quantitative analysis of endogenous jasmonoids in potato plant (*Solanum tuberosum* L.). *Biosci. Biotechnol. Biochem.* **64**, 2380–2387
 34. Ogawa, N., and Kobayashi, Y. (2012) Synthesis of the amino acid conjugates of *epi*-jasmonic acid. *Amino Acids* **42**, 1955–1966
 35. Nicolau, K. C., Estrada, A. A., Zak, M., Lee, S. H., and Safina, B. S. (2005) A mild and selective method for the hydrolysis of esters with trimethyltin hydroxide. *Angew. Chem. Int. Ed. Engl.* **44**, 1378–1382
 36. LeClere, S., Tellez, R., Rampey, R. A., Matsuda, S. P., and Bartel, B. (2002) Characterization of a family of IAA-amino acid conjugate hydrolases from *Arabidopsis*. *J. Biol. Chem.* **277**, 20446–20452
 37. VanDoorn, A., Bonaventure, G., Schmidt, D. D., and Baldwin, I. T. (2011) Regulation of jasmonate metabolism and activation of systemic signaling in *Solanum nigrum*. COI1 and JAR4 play overlapping yet distinct roles. *New Phytol.* **190**, 640–652
 38. Campanella, J. J., Larko, D., and Smalley, J. (2003) A molecular phylogenomic analysis of the ILR1-like family of IAA amidohydrolase genes. *Comp. Funct. Genomics* **4**, 584–600
 39. Toufighi, K., Brady, S. M., Austin, R., Ly, E., and Provard, N. J. (2005) The Botany Array Resource. e-Northern, expression angling, and promoter analyses. *Plant J.* **43**, 153–163
 40. Woldemariam, M. G., Onkokesung, N., Baldwin, I. T., and Galis, I. (2012) Jasmonoyl-L-isoleucine hydrolase 1 (JIH1) regulates jasmonoyl-L-isoleucine levels and attenuates plant defenses against herbivores. *Plant J.* **72**, 758–767
 41. Seto, Y., Hamada, S., Matsuura, H., Matsushige, M., Satou, C., Takahashi, K., Masuta, C., Ito, H., Matsui, H., and Nabeta, K. (2009) Purification and cDNA cloning of a wound inducible glucosyltransferase active toward 12-hydroxy jasmonic acid. *Phytochemistry* **70**, 370–379
 42. Ludwig-Müller, J. (2011) Auxin conjugates. Their role for plant development and in the evolution of land plants. *J. Exp. Bot.* **62**, 1757–1773
 43. Staswick, P. (2009) Plant hormone conjugation. A signal decision. *Plant Signal. Behav.* **4**, 757–759
 44. Bartel, B., and Fink, G. R. (1995) ILR1, an amidohydrolase that releases active indole-3-acetic acid from conjugates. *Science* **268**, 1745–1748

Jasmonate Conjugate Cleavage and Tuberonic Acid Formation

45. Todoroki, Y., Narita, K., Muramatsu, T., Shimomura, H., Ohnishi, T., Mizutani, M., Ueno, K., and Hirai, N. (2011) Synthesis and biological activity of amino acid conjugates of abscisic acid. *Bioorg. Med. Chem.* **19**, 1743–1750
46. Koo, A. J., Gao, X., Jones, A. D., and Howe, G. A. (2009) A rapid wound signal activates the systemic synthesis of bioactive jasmonates in *Arabidopsis*. *Plant J.* **59**, 974–986
47. Bhosale, R., Jewell, J. B., Hollunder, J., Koo, A. J., Vuylsteke, M., Michael, T., Hilson, P., Goossens, A., Howe, G. A., Browse, J., and Maere, S. (2013) Predicting gene function from uncontrolled expression variation among individual wild-type *Arabidopsis* plants. *Plant Cell*. doi:10.1105/tpc.113.112268